Wheel Slip Control for the Electric Vehicle With In-Wheel Motors: Variable Structure and Sliding Mode Methods

Dzmitry Savitski [ORCID], *Member, IEEE*, Valentin Ivanov [ORCID], *Senior Member, IEEE*, Klaus Augsburg, Tomoki Emmei [ORCID], *Student Member, IEEE*, Hiroyuki Fuse, Hiroshi Fujimoto, *Senior Member, IEEE*, and Leonid M. Fridman

Abstract—The article introduces four variants of the controller design for a continuous wheel slip control (WSC) system developed for the full electric vehicle equipped with individual in-wheel motors for each wheel. The study includes explanation of the WSC architecture, design of controllers, and their validation on road tests. The investigated WSC design variants use variable-structure proportional-integral, first-order sliding mode, integral sliding mode controllers as well as continuous twisting algorithm. To compare their functionality, a benchmark procedure is proposed based on several performance factors responsible for driving safety, driving comfort, and control quality. The controllers are compared by the results of validation tests done on low-friction road surface.

Index Terms—Continuous twisting algorithm (CTA), electric vehicle (EV), in-wheel motors (IWMs), sliding mode control, variable structure systems, wheel slip control (WSC).

I. INTRODUCTION

FULL electric vehicles (EVs) with individually controlled electric motors for each wheel are becoming a wide

D. Savitski is with the Arrival Germany GmbH, 75172 Pforzheim, Germany (e-mail: savitski@arrival.com).

V. Ivanov and K. Augsburg are with the Automotive Engineering Group, Technical University of Ilmenau, 98693 Ilmenau, Germany (e-mail: valentin.ivanov@tu-ilmenau.de; klaus.augsburg@tu-ilmenau.de).

T. Emmei, H. Fuse, and H. Fujimoto are with the Department of Advanced Energy, Graduate School of Frontier Sciences, The University of Tokyo, Kashiwa 277-8561, Japan (e-mail: enmei.tomoki14@ae.k.u-tokyo.ac.jp; fuse.hiroyuki17@ae.k.u-tokyo.ac.jp; fujimoto@k.u-tokyo.ac.jp).

L. M. Fridman is with the Department of Control and Robotics Engineering, National Autonomous University of Mexico, Mexico 04510, Mexico (e-mail: leonfrid54@hotmail.com).

Color versions of one or more of the figures in this article are available online at http://ieeexplore.ieee.org.

distribution in road transportation not only thanks to their environment-friendliness but also due to their agile and efficient motion dynamics. This was confirmed by many preliminary industrial studies, e.g., [1], [2], which have motivated further developments in EV motion control. Substantial advantages by designing of EV dynamics control systems can be provided by in-wheel motors (IWMs) as actuators in comparison with an internal combustion engine and friction brakes in conventional vehicles. These advantages are caused by the following factors: 1) IWM technology provides a quicker system response and has relatively high system bandwidth; 2) the output motor torque can be accurately measured from current that increase the control precision; and 3) all wheels can be controlled independently from each other allowing individual wheel torque control. As a result, new design principles and control architectures can be proposed for motion control systems in EVs with IWMs. Recent state-of-the-art surveys demonstrate that most of studies in this area are dedicated to torque vectoring, direct yaw control, and traction control systems [3], [4]. But the wheel slip control in a braking mode, despite its cardinal importance to any motion control systems, is still insufficiently addressed in published studies for the EVs with individually controlled electric motors. In many cases, the developers rather adopt algorithms taken from conventional antilock braking systems (ABS) and consider blended actuation of IWMs and friction brakes [5], [6] than propose WSC methods for a pure regenerative braking. However, exactly for this EV operational mode, the benefits of IWMs as actuators can be realized in a full measure. It concerns first of all the possibility to realize a continuous WSC that is opposite to a more common rule-based (RB) control approach.

The continuous WSC was initially proposed for decoupled brake-by-wire systems [7], [8] and demonstrated very precise tracking of reference wheel slip without pronounced brake torque oscillations typical of RB ABS. However, this approach was not deeply investigated during last decade, mainly due to limited use of brake-by-wire systems on mass-production cars. But for EVs, the relevant studies are gained a new impetus because on-board and IWMs allow efficient implementation of continuous wheel torque control.

The continuous WSC in EV can be realized in practice with different analytical approaches. Analysis of recent studies allows identifying three main major approaches in this regard. *The*

first group covers solutions based on more traditional nonlinear control methods as Lyapunov-based and proportional integral derivative (PID). One of the well-known approaches is based on so-called maximum transmissible torque estimation (MTTE) scheme allowing the controller design without the use of information about the vehicle velocity and tire-road friction [9]. The MTTE scheme with the proportional integral (PI) controller demonstrated good applicability for WSC on small EV with low operational velocities in a traction mode [10], however, such a design has been rarely studied for conventional passenger cars and for the braking mode. Another solution is proposed in the work [11] investigating the WSC, which uses the barrier Lyapunov function and is integrated with active suspension control. This method demonstrated sufficient braking performance but only in the simulation for a quarter car model. In general, it should be mentioned that only few WSC studies considered a full-scale validation on the mass-production cars. One of the recent experimental works in this regard has been performed for a full electric sport utility vehicle with four on-board motors, where a pure regenerative ABS were realized with gain-scheduled PI direct slip control with feed-forward and feedback control contributions [12]. The outcomes confirmed that continuous WSC with electric motors as actuators allows achieving simultaneous effect in high brake performance and improved driving comfort thanks to vehicle jerk damping.

The basic tool for *the second group* is model predictive control (MPC). A variant of a centralized MPC has been proposed in [13] for blended WSC with motors and friction brakes as redundant actuators. This variant demonstrated sufficient real-time applicability and good torque tracking in low-slip area. Simulation studies on nonlinear MPC-based WSC have been published in [14] (focus on uneven snow surface conditions), [15] (focus on blended ABS design), and [16] (focus on robustness against noise injection by the road profile). Some limitations of MPC are known regarding real-time performance; therefore, the MPC-based WSC on real vehicles is still rarely investigated. However, recent studies using hardware-in-the-loop technique confirmed sufficient performance of nonlinear MPC as a tool for continuous WSC [17].

The third group unites a variety of WSC methods based on sliding mode techniques. For example, the work [18] used sliding mode (SM) method for EV traction control with optimal slip seeking. A similar variant, but for an ABS mode, has been discussed in [19]. To increase robustness, some studies proposed integration of SM control technique with other methods. For instance, Verma *et al.* [20] introduced SM control combined with inertial delay control for estimating uncertainties at braking. Another example is provided by Zhang and Li [21], where a radial basis function neural network is added to SM WSC for the predefinition of optimal slip. An analysis of state-of-the-art solutions for WSC using SM methods allows identifying most common drawbacks of relevant studies: 1) their validation is mostly limited by simulation for a limited number of test cases; 2) optimal or reference slip is often selected in very high area $\lambda = 0.1...0.2$, even for low-friction surfaces, that does not correspond to real road conditions; and 3) the controllers demonstrate a chattering effect, particularly at low velocities.

Despite these drawbacks, the authors selected SM technique due to its robustness and relatively low computational costs for further study on WSC for EV with IWMs. It should be noted that there are also no clear recommendations in the literature regarding the selection of the most suitable SM strategy for EV control. In particular, analysis in [22] allows us to conclude that PI control proposes more effective wheel slip control than classical first-order SM and second-order SM. However, performed theoretical analysis in [23] indicates that integral sliding mode (ISM) is the most promising control over other SM controls. The latest conclusion is also confirmed in [24] and [25], though for the decoupled electro-hydraulic brake system. Therefore, the authors decided to design several concurrent variants of the controller with their benchmark by experimental results. The selected variants are as follows.

1) Variable structure PI (VSPI) as a method demonstrating integration of variable structure control techniques with the continuous PI control method.
2) The first-order SM, known for its issues with the chattering, to investigate IWM potentials as highly dynamic WSC actuator.
3) Integral SM recommended by other studies as a method demonstrating high robustness against delays and less overshooting.
4) SM with continuous twisting algorithm (CTA) characterized by the finite-time convergence of the control signal to the uncertainties. It should be especially noted that CTA approach is one of the recent advancements in SM control and there are no known experimental studies demonstrating its real-time application to such highly dynamic systems as EV WSC.

For these controller variants, the following objectives are formulated for the presented study:

1) to validate functionality of developed WSC variants using experiments on the proving ground in inhomogeneous and severe road surface conditions characterized by distinctive uncertainties;
2) to propose methodology for benchmark of different WSC variants and compare the developed systems using this methodology.

Next sections introduce how the proposed objectives and targets are achieved. Overall configuration and technical data of the target EV are given in Section II. Section III gives required introduction in wheel slip dynamics and its control targets. Then, the proposed continuous wheel slip control methods are explained in Section IV. The solution for the wheel slip estimation as an important WSC component is given Section V. The proposed continuous WSC methods are initially validated and compared in simulation studies described in Section V and, then, with real experiments presented in Section VI. Section VII concludes this article.

II. VEHICLE SPECIFICATION

The vehicle used in this article has been built at the University of Tokyo, Fig. 1, and is equipped with four individual outer-rotor-type IWMs, which adopt a principle of direct drive

Fig. 1. Vehicle demonstrator FPEV2-Kanon with four individual electric motors.

TABLE I
VEHICLE TECHNICAL DATA

Vehicle specification	
Vehicle type	FPEV2-Kanon
Full mass (kg)	847
Driveline	All-wheel drive
Wheelbase (m)	1.7
Track width (m)	1.3
Wheel radius (m)	0.302
Electric motors	
Front wheel maximal torque (Nm)	± 500 Nm
Rear wheel maximal torque (Nm)	± 530 Nm

system. It implies that reaction forces from the road are transmitted directly to the motors without gear reduction or backlash. Technical data of the test vehicle are given in Table I.

During the tests, the vehicle velocity is measured by the Corevit optical sensor. The dSPACE real-time platform with ds1003 processor board is installed on the vehicle for all required on-board control systems.

III. WHEEL SLIP DYNAMICS

The WSC algorithms developed in this study are using a single corner model, which can be described as follows:

$$\begin{cases} m\dot{V}_x = -F_x \\ J_w\dot{\omega}_w = F_x r_w - T_b \end{cases} \quad (1)$$

where V_x is the vehicle velocity, m is the mass of quarter vehicle, F_x is the tire longitudinal force, J_w is the wheel inertia, ω_w is the angular wheel velocity, r_w is the wheel radius, and T_b is the braking torque produced by electric motor.
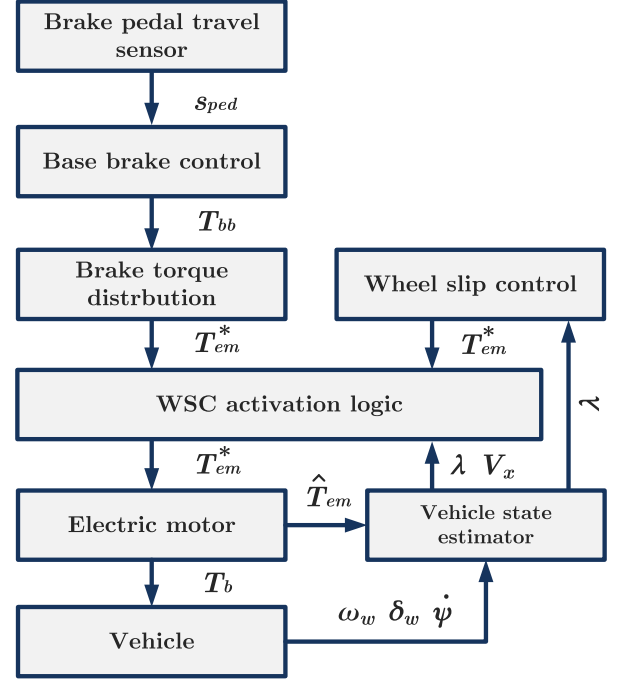

Fig. 2. Structure of the wheel slip controller.

Neglecting tire transient dynamics, the force F_x can be calculated as nonlinear function of the wheel slip λ

$$F_x = F_z \mu_{\text{road}}(\lambda) \quad (2)$$

where μ_{road} is the road coefficient of friction, and F_z is the vertical tire force.

For the longitudinal vehicle motion and braking mode, the wheel slip λ is calculated as

$$\lambda = \frac{\omega_w r_w - V_x}{V_x}. \quad (3)$$

Considering $V > 0$ and $\omega_w > 0$, the wheel slip dynamics can be described in general as

$$\dot{\lambda} = -\frac{1}{V_x}\left(\frac{1}{m}(1-\lambda) + \frac{r_w^2}{J_w}\right)F_z\mu_{\text{road}}(\lambda) + \frac{r_w}{J_w V_x}T_b. \quad (4)$$

The proposed interpretation of the wheel dynamics is sufficient for the design of the wheel slip control that was confirmed by the corresponding analysis done in [26]. However, it should be especially mentioned that the effect of the load distribution at the braking as well as eventual fluctuations of the road friction during the maneuver are handled as uncertainty in the controllers, which will be introduced in next section.

IV. WHEEL SLIP CONTROL

A. General Controller Structure

In the proposed structure of the wheel slip controller, Fig. 2, the overall base brake torque T_{bb} for the vehicle is computed from the driver demand, which can be defined through the brake pedal actuation dynamics, e.g., from the brake pedal displacement s_{ped}. The proposed WSC architecture for vehicle

with IWMs uses principle of direct slip control and generates electric motor torque demand T_{em}^* necessary for maintaining desired wheel slip λ^*. The WSC is being activated individually for each wheel when wheel slip λ is higher than reference λ^*. Deactivation happens if torque demand from distribution function is lower than the torque from WSC. Under this conditions, WSC or distributed torque demand are bypassed to the low-level electric motor controller. In this article, the reference wheel slip value is fixed at the value close to the optimum.

The structure includes also the state and parameter estimator block to compute the actual wheel slip λ and the estimated longitudinal wheel force $\hat{F}_x$ from the vehicle sensors measuring the wheel angular speed ω_w, steering wheel angle δ_w, and yaw rate $\dot{\psi}$. The reference wheel slip λ^* is calculated in the reference wheel slip generator block in accordance with the procedures described in [25]. Therefore, the wheel slip controller minimizes the error λ_e between the actual λ and reference λ^* wheel slip values

$$\lambda_e = \lambda^* - \lambda. \tag{5}$$

The investigated controller variants for this purpose are discussed in next sections.

B. VSPI Control

Assuming constant wheel slip reference $\lambda^* = 0$, representing T_{em} with PI control law and considering $\vartheta_2 = \lambda$, the system becomes the following closed-loop formulation:

$$\begin{cases} \dot{\vartheta}_1 = \vartheta_2 \\ \dot{\vartheta}_2 = -\dfrac{\lambda^* F_x}{mV_x} + \dfrac{(\vartheta_2 - 1)F_x}{V_x m} - \dfrac{r_w^2 F_x}{J_w V_x} \\ \quad + \dfrac{r_w}{J_w V_x} K_p \left(\vartheta_2 + \dfrac{1}{t_a} \vartheta_1 \right) \end{cases} \tag{6}$$

where ϑ_1 represents the integral of the wheel slip, and $\vartheta_2 = \lambda$ is the wheel slip.

Then, the state trajectories can be presented by the following equation, where the longitudinal tire force F_x can be calculated from a nonlinear steady-state tire model

$$\frac{d\vartheta_2}{d\vartheta_1} = -\frac{\lambda^* F_x + (\vartheta_2 - 1)F_x}{mV_x \vartheta_2} - \frac{r_w^2 F_x}{J_w V_x \vartheta_2} + \frac{r_w}{J_w V_x} K_p \left(1 + \frac{\vartheta_1}{t_a \vartheta_2} \right) \tag{7}$$

where K_p is the proportional control gain, and t_a is the tuning parameter of the integral part.

The state trajectories of this closed-loop system allow the designing control law for WSC. As it can be seen on the left of Fig. 3, constant gains of PI control produce not only inefficient solution in terms of brake force, but can also produce traction torque by electric motors. Considering these issues, VSPI control can be adjusted to have quicker dynamics in unstable area (higher P contribution and lower I), while slower control action should be produced in stable area (lower P contribution and higher I). Therefore, it is proposed to switch between control
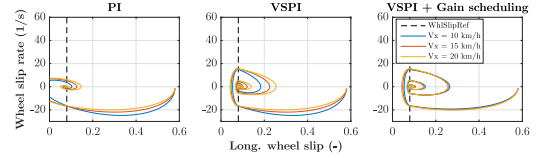

Fig. 3. State trajectories of wheel slip dynamics with PI and VSPI WSC: PI control without switching logic (left) switching gains at reference wheel slip (left) and gain scheduling of PI gain in stable and unstable areas (right).

gains when the wheel slip passes reference value λ^*

$$K_p = \begin{cases} K_{p1}, & \text{if } \lambda < \lambda^* \\ K_{p2}, & \text{otherwise} \end{cases} \tag{8}$$

$$t_a = \begin{cases} t_{a1}, & \text{if } \lambda < \lambda^* \\ t_{a2}, & \text{otherwise} \end{cases} \tag{9}$$

where K_{p1}, K_{p2} are proportional control gains, and t_{a1}, t_{a2} are tuning parameters of the integral control part. Presented equations show how the gains are switched depending on the wheel slip position in relation to the stability point of force-wheel slip diagram.

The resulting system behavior is presented on the phase plane in middle of Fig. 3. In this case, the system is driven to the origin with a higher wheel slip rate in the area over the optimal slip to avoid wheel locking. The wheel slip is held close to the optimum in the area under the reference.

The system trajectories from Fig. 3 show that dynamics depends on the vehicle velocity. Therefore, the scheduling of P and I gains of VSPI control should be performed to achieve a predictable system response. The right-hand side of Fig. 3 displays the trajectories after preliminary setting of the control gains scheduled by the vehicle velocity variation. This provides predictable system behavior and allows obtaining the gain scheduling curves for K_p and t_a before experiments.

Additional tuning of the controller gains has been performed using commercial vehicle dynamics simulation environment. A set of straight-line braking maneuvers has been considered, where initial velocity of the vehicle has been varied from 10 to 120 km/h with the step of 10 km/h. For each velocity case, offline optimization was performed to find optimal values of the K_{p1}, K_{p2} and t_{a1}, t_{a2} using the genetic optimization algorithm [27]. Cost function for the optimization procedure was formulated as follows:

$$J_{\text{cost}} = w_1 \frac{s_{\text{dist}}}{s_{\text{max}}} + w_2 \sqrt{\frac{\sum_{i=1}^{N} (\lambda^* - \lambda_i)^2}{N - 1}} + w_3 \sqrt{\frac{\sum_{i=1}^{N} \left(a_x - \frac{1}{N}\sum_{i=1}^{N} a_x\right)^2}{N - 1}} \tag{10}$$

where s_{dist} is the braking distance, s_{max} is the maximal braking distance obtained by considering vehicle without ABS, a_x is the vehicle longitudinal deceleration, and N is the number of measuring points considering sampling rate of 1 ms.

The highest priority across driving safety, driving comfort, and control quality has been given to the safety, and the lowest

has been assigned to the comfort. This is possible to be done by adjustment of corresponding weight coefficient w_1, w_2, and w_3, respectively.

C. First-Order Sliding Mode (FOSM) Control

For this WSC variant, sliding variable σ is defined the same as the control error

$$\sigma = \lambda_e = \lambda^* - \lambda. \tag{11}$$

The control law for the classical sliding mode approach is defined as

$$T_{em} = -K_{\text{fosm}}\text{sign}(\sigma) \tag{12}$$

with the control gain K_{fosm} as a positive constant.

Remark: To avoid chattering, which is critical for mechanical systems, sign function can be replaced with its following approximation [28]:

$$\hat{\text{sign}}[x(t)] = \frac{x(t)}{|x(t)| + \epsilon} \tag{13}$$

with a reasonably small value of $\epsilon > 0$. Higher values of ϵ can follow to the loss of control performance, which is characterized by occurrence of static error in presence of matched disturbances [29].

The system uncertainty $h(x)$ to be used in (13) can be obtained from the wheel slip dynamics

$$\dot{\lambda} = B(x)(-r_w F_z \mu_{\text{road}}(\lambda) + T_{em} + T_{b,\text{unc}}) \tag{14}$$

where $B(x)$ is the input matrix. Then, the system uncertainty $h(x)$ is determined by

$$h(x) = -r_w F_z \mu_{\text{road}}(\lambda) + T_{b,\text{unc}}. \tag{15}$$

Finally, referring to [30], the following inequality should be satisfied:

$$K_{\text{fosm}} \geq |h_{\text{max}}|. \tag{16}$$

Despite application of FOSM as the WSC is known from various literature sources [31], this control technique was rarely tested on the real EVs due to the issues with chattering. Despite this disadvantage of the FOSM method, its feasibility by using IWMs with a relatively high system bandwidth will be checked and compared to other control techniques from this section.

D. Integral Sliding Mode

The ISM control method can ensure less chattering and also provide compensation both of matched and unmatched disturbances. In the case of ISM implementation, the wheel slip dynamics should be presented in the following form considering uncertainties:

$$\dot{x} = f(x) + B(x)u + h(x), \text{where } |h(x)| < h_{\text{max}}. \tag{17}$$

The contributions of the ISM control effort are

$$T_{em} = T_c + T_d \tag{18}$$

where T_c and T_d are continuous and discrete control contributions.

It is proposed in this article to use the VSPI controller as the continuous part. The discontinuous part can be presented as

$$T_d = -K_{\text{ism}}\text{sign}(s) \tag{19}$$

where K_{ism} is the control gain of the discontinuous part.

The discontinuous control is, then, filtered for reduced chattering and a smoother control action. Following recommendations from [32], a first-order linear filter can be used for this purpose. Its tuning as well as the selection of the time constant τ_{sw} are performed under a condition to avoid distorting the slow component of the switched action

$$T_d = \dot{T}_d^{\text{filt}}\tau_d + T_d^{\text{filt}}. \tag{20}$$

Furthermore, the sliding surface consists of the two parts

$$\sigma = \sigma_0 + z \tag{21}$$

where z is the integral term, and $\sigma_0 = \lambda^* - \lambda$ is the sliding variable.

On the next step, the derivative of the reference wheel slip is subtracted that yields

$$\Delta\dot{\lambda} = \dot{\lambda} - \dot{\lambda}^* = -\dot{\lambda}^* - B(x)r_w F_z \mu(\lambda)$$
$$+ B(x)u + B(x)T_{w,\text{unc}}. \tag{22}$$

Here, the known variable is the reference wheel slip λ^*, $f(x) = \lambda^*$, and the disturbance is the additional wheel torque $T_{w,\text{unc}}$.

It can be finally derived that the auxiliary variable z equals to

$$\dot{z} = -\frac{\partial\sigma_0}{\partial(\lambda - \lambda^*)}(-\dot{\lambda}^* + B(x)(u_{\text{ism}} - u_d))$$
$$= \dot{\lambda}^* - B(x)(u - u_d). \tag{23}$$

The proof of stability of this ISM structure can be found in [25].

E. Continuous Twisting Algorithm

CTA relates to the sliding mode control methods and known by its benefits in terms of disturbances compensation and solving of chattering issue [33] and [34]. These advantages of the method motivated its application for the WSC system, which has similar design requirements: providing smooth wheel slip tracking and robustness to disturbances. This control technique produces third-order sliding mode in a relation system state. Hence, this method cannot be naturally applied to the considered system. As the solution, system order can be auxiliary increased. According to definition of relative degree of freedom ρ [35], this corresponds to the minimum order of the time derivative of sliding variable s^ρ, where control input T_{em} explicitly appears [23]. Computing first and second derivatives of the sliding variable,

following representation of the system is obtained:

$$
\begin{cases}
\dot{s} = -\dfrac{1}{V_x}\dfrac{r_w^2}{J_w}F_x + \dfrac{r_w}{J_w V_x}T_{\text{em}} \\[2mm]
\ddot{s} = \ddot{\lambda}^* - \dfrac{r_w^2 \dot{F}_x}{J_w V_x} + \dfrac{r_w^2 F_x \dot{V}_x}{J_w V_x^2} - \dfrac{\dot{F}_x r_w \omega}{m V_x^2} - \dfrac{F_x r_w \dot{\omega}}{m V_x^2} \\[2mm]
+ \dfrac{2 F_x r_w \omega \dot{V}_x}{m V_x^3} - \dfrac{r_w \dot{V}_x}{J_w V_x^2}T_{\text{em}} + \dfrac{r_w}{J_w V_x}\dot{T}_{\text{em}}
\end{cases} . \quad (24)
$$

Right-hand side of the second equation in this system includes several components, which cannot be estimated in a reliable way. Hence, it is proposed to consider them as the system disturbance $w(t)$. Therefore, this auxiliary system can be presented in a general form as

$$
\begin{cases}
\dot{\zeta}_1(t) = \zeta_2(t) \\
\dot{\zeta}_2(t) = w(t) + g(t)\nu(t)
\end{cases} . \quad (25)
$$

Presented system has two auxiliary states $\zeta_1 = s$ and $\zeta_2 = \dot{s}$ and ν represents auxiliary control input. Therefore, control effort T_{em} is expressed as the integral of the auxiliary control input, which provides continuous control input

$$
T_{\text{em}} = \int_{\tau_1}^{\tau_2} \nu(t). \quad (26)
$$

After obtaining this system description, control problem can be formulated. This is concluded in driving the state ζ (which is equal to the wheel slip error λ_e) to the origin despite disturbances that affect the system. To solve this problem, aforementioned CTA can be applied as in [36]

$$
\begin{cases}
\nu(\zeta) = -K_{\text{cta},1}\lceil\zeta_1\rceil^{\frac{1}{3}} - K_{\text{cta},2}\lceil\zeta_2\rceil^{\frac{1}{2}} + \eta \\
\dot{\eta} = -K_{\text{cta},3}\lceil\zeta_1\rceil^{0} - K_{\text{cta},4}\lceil\zeta_2\rceil^{0}
\end{cases} \quad (27)
$$

where notation $\lceil\cdot\rceil^{\gamma}$ means $\text{sign}(\cdot)\cdot|\cdot|^{\gamma}$.

To guarantee stability of CTA control strategy, offline optimization of control gains can be performed. Method, described in [36], was utilized for this purpose to confirm stability of the system.

V. SIMULATION RESULTS

Before the implementation of the proposed wheel slip controllers on the vehicle demonstrator, they were investigated in simulation to tune the parametrization. The simulation scenario corresponds to the test conditions of the proving track at the University of Tokyo. The track has an inhomogeneous low-friction surface composed from wet plastic sheets. For this surface, the reference wheel slip was set as $\lambda^* = 0.04$ for the experimentally defined average tire-road friction coefficient $\mu = 0.21$. The initial braking velocity is 30 km/h for all tests. The simulation diagrams are given in Figs. 4 and 5, where the indices mark the wheels: FL—for the front left, FR—for the front right, RL—for the rear left, and RR—for the rear right. The analysis of simulation results allowed us to deduce the following observations.

The VSPI control produces the highest value of the first wheel slip peak that is caused by the integral part of the controller.
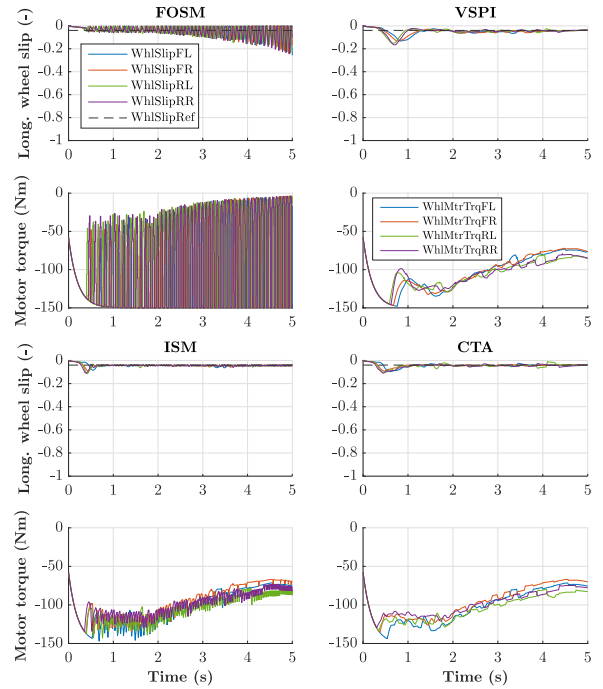

Fig. 4.   Wheel slip control with IWMs in low road friction conditions.
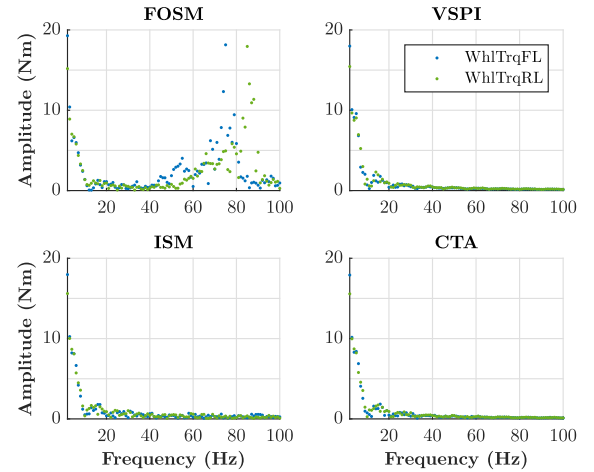

Fig. 5.   Distribution of the brake torque demand in frequency spectrum.

But, after the reaching of control setpoint, the further process is characterized by sufficiently smooth and precise tracking of the reference slip. The FOSM control demonstrates better agility because the reference wheel slip is reached within a shorter time as compared to other WSC variants. However, the overall process is suffering from considerable chattering that can be seen on the motor torque behavior, which is characterized by oscillations with high amplitude and frequency (approx. 50 to 90 Hz). However, the IWMs used in this study provide a direct torque transmission to the wheels and have sufficient performance to realize the FOSM approach without damages of driveline components. Such drawbacks, as the high first control peak by VSPI method and the considerable chattering by the

TABLE II
WSC NUMERICAL EVALUATION FOR THE BRAKING IN
LOW FRICTION CONDITIONS WITH IWMS

Evaluation criterion	RB	FOSM	VSPI	ISM	CTA
Control quality					
Wheel slip FL RMSD, (-)	-	0.03	0.03	0.01	0.01
Wheel slip FR RMSD, (-)	-	0.04	0.03	0.01	0.01
Wheel slip RL RMSD, (-)	-	0.03	0.03	0.01	0.01
Wheel slip RR RMSD, (-)	-	0.03	0.03	0.01	0.01
Wheel slip first peak FL, (-)	0.45	0.06	0.13	0.08	0.09
Wheel slip first peak FR, (-)	0.42	0.05	0.13	0.09	0.09
Wheel slip first peak RL, (-)	0.27	0.06	0.15	0.11	0.10
Wheel slip first peak RR, (-)	0.38	0.06	0.17	0.11	0.11
Driving safety					
Braking distance, (m)	23.2	23.7	21.0	20.9	20.9
Driving comfort					
Jerk STD, (m/s^3)	2.3	4.7	0.4	0.4	0.4

Fig. 6. Wheel slip control with IWMs in low road friction conditions.

FOSM method, are being eliminated in the case of the ISM wheel slip controller. To achieve this effect, the ISM controller has been tuned and its low-pass filter was designed with relatively high cutoff frequency applicable for IWMs. The CTA control is possessed of described advantages of the ISM variant but has, in addition, a smoother dynamics of the motor torque demand. This means that this control operates in relatively small frequencies compared to the other control approaches, see Fig. 5.

To assess benefits of developed WSC strategies, RB approach [25] was used for comparison. For fair comparison of control methods, RB approach was used in combination with IWMs. Numerical evaluation of each control strategy is summarized in Table II.

These simulation studies allowed to fix the final design of all four WSC variants and to realize them on the vehicle demonstrators for the proving track experiment. Their results are discussed in next section.

VI. EXPERIMENTAL RESULTS

The experimental program considered the following factors. The gains for four tested WSC variants were selected on the basis of previous simulation studies with minimal tuning during the tests. Due to track limitations, vehicle velocity around 25 k/h was considered during vehicle tests. The proving track surface was properly wetted before each trial to guarantee the consistency of experiments and reach $\mu_{\text{road}} \approx 0.2$. The braking maneuverer were repeated about 40 times for each controller variant. The experimental results are given in Fig. 6. The analysis of the tests allowed us to draw the following observations.

VSPI control showed the worst tracking performance for the front and rear wheels. Switching of the control gains at reference wheel slip point allows compensating difference in system dynamics. However, this leads to more oscillatory behavior of requested wheel torque. As a consequence, the first peak is
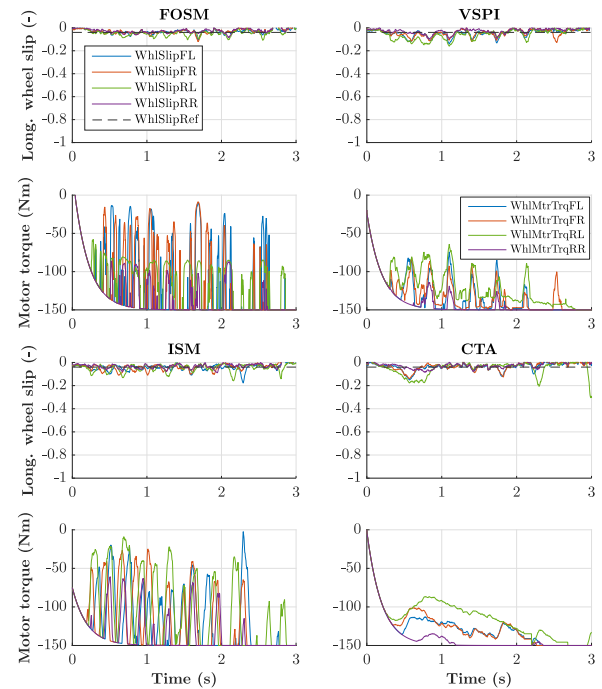
relatively high and the system oscillates with such amplitude during the whole braking event. Despite this fact, the ride quality did not suffer from these oscillations due to their relatively low modulation frequency.

For the FOSM control, compared to the simulation results with significant chattering and higher deviation from the reference value, these effect were attenuated during road tests. Such high-frequency modulation of braking torque was not bypassed by tires, which have first-order dynamics with lower cutoff frequency. This effect led to better tracking performance than in simulation, where transient tire dynamics were not experimentally validated for this type of vehicle. Among other control approaches, FOSM has shown the most agile reaction during initial phase of WSC activation and the first peak for the front and rear wheels has the lowest value. Nevertheless, FOSM still produces oscillatory torque behavior, which has a negative influence on the ride quality.

With PI control as the continuous control action, the ISM approach demonstrated much better results in terms of tracking performance and system adaptability compared to VSPI control. Such system adaptability was guaranteed by discrete control part responsible for disturbance rejection. ISM control provided ride quality comparable with VSPI and CTA approaches.

The most precise and smooth control action was produced by CTA algorithm due to the presence of integral control part and subsequent integration of virtual input. Theoretically, this approach handles variation of the road conditions and vertical load during the emergency that is confirmed experimentally for this case. However, presence of the integral part leads to significantly slower system reaction at the WSC activation stage. Hence, CTA has the highest first peak for front and rear wheels. Nevertheless, such progressive variation has huge benefits in terms of the ride

TABLE III
WSC NUMERICAL EVALUATION FOR THE BRAKING IN
LOW FRICTION CONDITIONS WITH IWMS

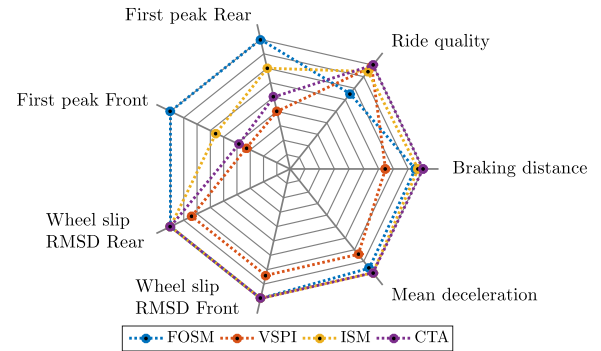| Evaluation criterion	FOSM	VSPI	ISM	CTA
Control quality				
Wheel slip FL RMSD, (-)	0.02	0.03	0.03	0.03
Wheel slip FR RMSD, (-)	0.03	0.03	0.02	0.02
Wheel slip RL RMSD, (-)	0.03	0.04	0.03	0.04
Wheel slip RR RMSD, (-)	0.03	0.03	0.02	0.02
Wheel slip first peak FL, (-)	0.08	0.12	0.10	0.15
Wheel slip first peak FR, (-)	0.06	0.11	0.11	0.14
Wheel slip first peak RL, (-)	0.09	0.15	0.13	0.18
Wheel slip first peak RR, (-)	0.06	0.1	0.07	0.08
Driving safety				
Mean deceleration, (m/s^2)	1.9	1.6	2.0	2.0
Braking distance, (m)	13.1	16.2	12.8	12.3
Driving comfort				
Deceleration STD, (m/s^2)	0.76	0.59	0.62	0.58

Fig. 7. Experimental comparison of developed WSC control strategies for the vehicle with IWMs. Note: Maximal value of the presented normalized metrics is 100% for each indicator that corresponds to the best performance.

quality compared to torque modulation: CTA provides lowest longitudinal vehicle jerk during emergency braking.

The final benchmark of the developed controllers is proposed on the basis of the assessment criteria, which evaluate the functionality of WSC by performance indicators related to the vehicle dynamics. These assessment criteria are commonly used in industrial practice [37], [38] by designing the traction and braking control systems:

1) braking distance and mean deceleration to evaluate braking performance;
2) vehicle jerk to evaluate ride quality;
3) peak value of the initial WSC control cycle to evaluate WSC agility and adaptability in terms of wheel slip dynamics;
4) wheel slip RMSD to evaluate the system performance by tracking the reference slip ratio.

The listed criteria are usually normalized to provide a comparison in percentages.

The test results are summarized in Table III and presented as normalized criteria on the radar plot in Fig. 7. The following observations can be done on the analysis of these data.

1) FOSM has the most agile reaction in WSC mode providing the lowest first peak.
2) Compared to the simulation results, FOSM braking torque was filtered by tire longitudinal dynamics, which resulted in precise wheel slip tracking.
3) Chattering in FOSM produced high-frequency braking torque demand, which negatively influenced ride quality during the WSC braking.
4) VSPI control produced the worst results in terms of control and braking performance due to more oscillatory brake torque demand modulation.

5) CTA can provides WSC solution applicable not only for IWMs, but also to brake actuators with slower dynamics; this is determined by smooth and progressive variation of the braking torque demand.

VII. CONCLUSION

The presented work investigated four methods for the wheel slip control using the sliding mode technique. These methods were studied in simulation and experiment for full EV with IWMs for each wheel. The following conclusions can be done for each method from the analysis of obtained results.

1) Compared to the classical PI control formulation, the VSPI control keeps the wheel slip in narrow area around the reference value during the whole braking process.
2) VSPI control allows compensating unmatched disturbances, which are strongly dependent on the vehicle velocity. This compensation can be realized with the proposed gain scheduling method based on the nonlinear wheel slip dynamics model.
3) FOSM has an advantage for the IWM control in terms of easy tuning. However, the WSC process with FOSM method is characterized by noticeable torque oscillations that can be considered as a disadvantage from viewpoint of the driving comfort.
4) As in the VSPI case, the ISM control can compensate unmatched uncertainties. In addition, the ISM-based WSC operation has less oscillatory behavior and better braking performance as compared to VSPI and FOSM variants.
5) The CTA provides smooth control signal and can be potentially applied to the brake systems with a lower bandwidth. However, tuning of this method is relatively sophisticated. Nevertheless, the WSC with the CTA formulation achieved the best braking efficiency in both simulation and experiment.

Summarizing, it should be concluded that the investigated sliding mode techniques demonstrated promising results for the WSC functions realized in EV with IWMs. In future works, the authors are planning to advance the application of four developed methods to further complex tasks related to the stability, ride, and integrated chassis control.

REFERENCES

[1] S. Murata, "Innovation by in-wheel-motor drive unit," *Veh. Syst. Dyn.*, vol. 50, no. 6, pp. 807–830, 2012. [Online]. Available: https://doi.org/10.1080/00423114.2012.666354

[2] E. Katsuyama, "Decoupled 3d moment control using in-wheel motors," *Veh. Syst. Dyn.*, vol. 51, no. 1, pp. 18–31, 2013. [Online]. Available: https://doi.org/10.1080/00423114.2012.708758

[3] H. Kanchwala, P. L. Rodriguez, D. A. Mantaras, J. Wideberg, and S. Bendre, "Obtaining desired vehicle dynamics characteristics with independently controlled in-wheel motors: State of art review," *SAE Int. J. Passenger Cars-Mech. Syst.*, vol. 10, no. 2017-01-9680, pp. 413–425, 2017.

[4] V. Ivanov, D. Savitski, and B. Shyrokau, "A survey of traction control and antilock braking systems of full electric vehicles with individually controlled electric motors," *IEEE Trans. Veh. Technol.*, vol. 64, no. 9, pp. 3878–3896, Sep. 2015.

[5] B. Wang, X. Huang, J. Wang, X. Guo, and X. Zhu, "A robust wheel slip ratio control design combining hydraulic and regenerative braking systems for in-wheel-motors-driven electric vehicles," *J. Franklin Inst.*, vol. 352, no. 2, pp. 577–602, 2015.

[6] M. S. Basrah, E. Siampis, E. Velenis, D. Cao, and S. Longo, "Wheel slip control with torque blending using linear and nonlinear model predictive control," *Vehicle Syst. Dyn.*, vol. 55, no. 11, pp. 1665–1685, 2017. [Online]. Available: https://doi.org/10.1080/00423114.2017.1318212

[7] S. B. Choi, "Antilock brake system with a continuous wheel slip control to maximize the braking performance and the ride quality," *IEEE Trans. Control Syst. Technol.*, vol. 16, no. 5, pp. 996–1003, Sep. 2008.

[8] S. Semmler, R. Isermann, R. Schwarz, and P. Rieth, "Wheel slip control for antilock braking systems using brake-by-wire actuators," SAE Technical Paper 2003-01-0325, pp. 1–8, 2003, doi: 10.4271/2003-01-0325.

[9] Dejun Yin and Yoichi Hori, "A new approach to traction control of EV based on maximum effective torque estimation," in *Proc. 34th Annu. Conf. IEEE Ind. Electron.*, Nov. 2008, pp. 2764–2769.

[10] J. Hu, D. Yin, Y. Hori, and F. Hu, "Electric vehicle traction control: A new MTTE methodology," *IEEE Ind. Appl. Mag.*, vol. 18, no. 2, pp. 23–31, Mar. 2012.

[11] J. Zhang, W. Sun, and H. Jing, "Nonlinear robust control of antilock braking systems assisted by active suspensions for automobile," *IEEE Trans. Control Syst. Technol.*, vol. 27, no. 3, pp. 1352–1359, May 2019.

[12] D. Savitski, V. Ivanov, B. Shyrokau, J. De Smet, and J. Theunissen, "Experimental study on continuous ABS operation in pure regenerative mode for full electric vehicle," *SAE Int. J. Passenger Cars-Mech. Syst.*, vol. 8, no. 2015-01-9109, pp. 364–369, 2015.

[13] C. Satzger, R. de Castro, A. Knoblach, and J. Brembeck, "Design and validation of an MPC-based torque blending and wheel slip control strategy," in *Proc. IEEE Intell. Veh. Symp. (IV)*, Jun. 2016, pp. 514–520.

[14] Y. Ma, J. Zhao, H. Zhao, C. Lu, and H. Chen, "MPC-based slip ratio control for electric vehicle considering road roughness," *IEEE Access*, vol. 7, pp. 52405–52413, 2019.

[15] M. S. Basrah, E. Siampis, E. Velenis, D. Cao, and S. Longo, "Wheel slip control with torque blending using linear and nonlinear model predictive control," *Veh. Syst. Dyn.*, vol. 55, no. 11, pp. 1665–1685, 2017.

[16] F. Pretagostini, B. Shyrokau, and G. Berardo, "Anti-lock braking control design using a nonlinear model predictive approach and wheel information," in *Proc. IEEE Int. Conf. Mechatronics*, Mar. 2019, vol. 1, pp. 525–530.

[17] D. Tavernini *et al.*, "An explicit nonlinear model predictive ABS controller for electro-hydraulic braking systems," *IEEE Trans. Ind. Electron.*, to be published, doi: 10.1109/TIE.2019.2916387.

[18] K. Han, M. Choi, B. Lee, and S. B. Choi, "Development of a traction control system using a special type of sliding mode controller for hybrid 4WD vehicles," *IEEE Trans. Veh. Technol.*, vol. 67, no. 1, pp. 264–274, Jan. 2018.

[19] K. Han, B. Lee, and S. B. Choi, "Development of an antilock brake system for electric vehicles without wheel slip and road friction information," *IEEE Trans. Veh. Technol.*, vol. 68, no. 6, pp. 5506–5517, Jun. 2019.

[20] R. Verma, D. Ginoya, P. Shendge, and S. Phadke, "Slip regulation for anti-lock braking systems using multiple surface sliding controller combined with inertial delay control," *Veh. Syst. Dyn.*, vol. 53, no. 8, pp. 1150–1171, 2015.

[21] J. Zhang and J. Li, "Adaptive backstepping sliding mode control for wheel slip tracking of vehicle with uncertainty observer," *Meas. Control*, vol. 51, no. 9-10, pp. 396–405, 2018.

[22] S. De Pinto, C. Chatzikomis, A. Sorniotti, and G. Mantriota, "Comparison of traction controllers for electric vehicles with on-board drivetrains," *IEEE Trans. Veh. Technol.*, vol. 66, no. 8, pp. 6715–6727, Aug. 2017.

[23] G. P. Incremona, E. Regolin, A. Mosca, and A. Ferrara, "Sliding mode control algorithms for wheel slip control of road vehicles," in *Proc. Am. Control Conf.*, 2017, pp. 4297–4302.

[24] D. Savitski, D. Schleinin, V. Ivanov, and K. Augsburg, "Individual wheel slip control using decoupled electro-hydraulic brake system," in *Proc. 43rd Annu. Conf. IEEE Ind. Electron. Soc.*, Oct. 2017, pp. 4055–4061.

[25] D. Savitski, D. Schleinin, V. Ivanov, and K. Augsburg, "Robust continuous wheel slip control with reference adaptation: Application to the brake system with decoupled architecture," *IEEE Trans. Ind. Informat.*, vol. 14, no. 9, pp. 4212–4223, Sep. 2018.

[26] S. M. Savaresi and M. Tanelli, *Active Braking Control Systems Design for Vehicles*. Berlin, Germany: Springer, 2010.

[27] R. Schaefer, *Foundations of Global Genetic Optimization*, vol. 74. Berlin, Germany: Springer, 2007.

[28] G. Ambrosino, G. Celentano, and F. Garofalo, "Robust model tracking control for a class of nonlinear plants," *IEEE Trans. Autom. Control*, vol. AC-30, no. 3, pp. 275–279, Mar. 1985.

[29] D. Efimov, A. Polyakov, L. Fridman, W. Perruquetti, and J.-P. Richard, "Delayed sliding mode control," *Automatica*, vol. 64, pp. 37–43, 2016.

[30] J. Dávila, L. Fridman, and A. Ferrara, "Introduction to sliding mode control," in *Sliding Mode Control Vehicle Dynamics*, 2017, Ch. 1, pp. 1–32.

[31] C. Unsal and P. Kachroo, "Sliding mode measurement feedback control for antilock braking systems," *IEEE Trans. Control Syst. Technol.*, vol. 7, no. 2, pp. 271–281, Mar. 1999.

[32] V. I. Utkin, *Sliding Modes in Control and Optimization*. Berlin, Germany: Springer, 2013.

[33] V. Torres-González, T. Sanchez, L. M. Fridman, and J. A. Moreno, "Design of continuous twisting algorithm," *Automatica*, vol. 80, pp. 119–126, 2017.

[34] T. Sanchez, J. A. Moreno, and L. M. Fridman, "Output feedback continuous twisting algorithm," *Automatica*, vol. 96, pp. 298–305, 2018.

[35] G. Bartolini, A. Pisano, E. Punta, and E. Usai, "A survey of applications of second-order sliding mode control to mechanical systems," *Int. J. Control*, vol. 76, nos. 9/10, pp. 875–892, 2003.

[36] V. Torres-González, L. M. Fridman, and J. A. Moreno, "Continuous twisting algorithm," in *Proc. IEEE 54th Ann. Conf. Decis. Control*, 2015, pp. 5397–5401.

[37] D. Savitski *et al.*, "The new paradigm of an anti-lock braking system for a full electric vehicle: Experimental investigation and benchmarking," *Proc. Inst. Mech. Eng., Part D: J. Automobile Eng.*, vol. 230, no. 10, pp. 1364–1377, 2016.

[38] H. A. Hamersma and P. S. Els, "ABS performance evaluation taking braking, stability and steerability into account," *Int. J. Veh. Syst. Model. Testing*, vol. 12, nos. 3/4, pp. 262–283, 2017.

Dzmitry Savitski (S'12–M'18) received the Dipl.-Ing. degree in automotive engineering from Belarusian National Technical University, Minsk, Belarus, in 2011, and Dr.-Ing. degree in automotive engineering from the Technical University of Ilmenau, Ilmenau, Germany, in 2019.

From 2009 to 2011, he was a Research Assistant with the Division for Computer Vehicle Design, Joint Institute of Mechanical Engineering, Minsk. From 2011 to 2018, he was working as a Research Fellow with Automotive Engineering Group, Technical University of Ilmenau, Germany, focusing on the vehicle dynamics and chassis control systems. In 2018, he joined Knorr-Bremse Commercial Vehicle Systems GmbH, Schwieberdingen, Germany, as a Development Engineer working on the topics of vehicle stability control for highly automated trucks. He is currently a Lead Engineer with Arrival Germany GmbH, Dortmund, Germany, coordinating control software development for the X-by-Wire chassis systems.

Dr. Savitski is a Member of the Association of German Engineers, the Society of Automotive Engineers, and the Tire Society.

Valentin Ivanov (M'13–SM'15) received the Ph.D. and D.Sc. degrees in automotive engineering from Belarusian National Technical University, Minsk, Belarus, in 1997 and 2006, respectively, and the Dr.-Ing. habil. degree in automotive engineering from the Technical University of Ilmenau, Ilmenau, Germany, in 2017.

From 1995 to 2007, he was consequently an Assistant Professor, an Associated Professor, and a Full Professor with the Department of Automotive Engineering, Belarusian National Technical University. In July 2007, he became an Alexander von Humboldt Fellow, and in July 2008, he became a Marie Curie Fellow with the Technical University of Ilmenau. He is currently EU Project Coordinator with the Automotive Engineering Group, Technical University of Ilmenau. His research interests include vehicle dynamics, electric vehicles, automotive control systems, chassis design, and fuzzy logic.

Prof. Ivanov is an Society of Automotive Engineers (SAE) Fellow and a Member of the Society of Automotive Engineers of Japan, the Association of German Engineers, the International Federation of Automatic Control (Technical Committee "Automotive Control"), and the International Society for Terrain-Vehicle Systems.

Klaus Augsburg received the Dr.-Ing. degree in automotive engineering from the Dresden University of Technology, Dresden, Germany, in 1985.

From 1984 to 1993, he worked in industry on leading engineer positions, and then, as a Senior Research Assistant with the Dresden University of Technology, Dresden, Germany, in 1993–1999. In 1999, he became a Full Professor and the Chair of the Automotive Engineering Group, Technical University of Ilmenau, Ilmenau, Germany. He is also the Chairman of Workgroup Automotive Engineering Verein Deutscher Ingenieure (VDI) Thringen and the Chief Executive Officer of Steinbeis-Transferzentrum Fahrzeugtechnik. He founded the Thuringian Centre of Innovation in Mobility in 2011, where he is coordinating public research projects and bilateral projects with industrial partners.

Prof. Augsburg is a Member of the Association of German Engineers.

Tomoki Emmei (S'15) received the B.S. and M.S. degrees in science from the University of Tokyo, Tokyo, Japan, in 2015 and 2017, respectively. He is currently working toward the Ph.D. degree with the Department of Electrical Engineering and Information Systems, the University of Tokyo.

He is also a Research Fellow with the Japan Society for the Promotion of Science from 2018 (JSPS-DC2). His research interest includes motion control and electric vehicle control.

Mr. Emmei received the IEEJ Young Researcher's Award in 2015 and the Dean's Award for Outstanding Achievement from the Graduate School of Frontier Sciences and Faculty of Engineering, the University of Tokyo in 2017 and 2015 respectively.

Hiroyuki Fuse received the B.Eng. degree in electrical and electronic engineering from the Tokyo Institute of Technology, Tokyo, Japan, in 2017, and the M.S. degree in advanced energy from the University of Tokyo, Tokyo, Japan, in 2019. He is currently working toward the Ph.D. degree with the Department of Advanced Energy, the University of Tokyo.

His current research interests include vehicle dynamics, and motion control of electric vehicle.

Mr. Fuse received the JSAE Graduate School Research Award from in 2019, IEEJ Excellent Presentation Award in 2019, and the Deans Award for Outstanding Achievement from the Graduate School of Frontier Sciences and Faculty of Engineering, the University of Tokyo in 2019. He is a Student Member of IEE of Japan and Society of Automotive Engineers (SAE) of Japan, respectively.

Hiroshi Fujimoto (S'99–M'01–SM'12) received the Ph.D. degree in electrical engineering from the Department of Electrical Engineering, University of Tokyo, Tokyo, Japan, in 2001.

In 2001, he joined the Department of Electrical Engineering, Nagaoka University of Technology, Niigata, Japan, as a Research Associate. From 2002 to 2003, he was a Visiting Scholar with the School of Mechanical Engineering, Purdue University, West Lafayette, IN, USA. In 2004, he joined the Department of Electrical and Computer Engineering, Yokohama National University, Yokohama, Japan, as a Lecturer and he became an Associate Professor in 2005. He is currently an Associate Professor with the Department of Advanced Energy, Graduate School of Frontier Sciences, University of Tokyo since 2010. His research interests include control engineering, motion control, nano-scale servo systems, electric vehicle control, motor drive, visual servoing, and wireless motors.

Prof. Fujimoto received the Best Paper Awards from the IEEE Transactions on Industrial Electronics in 2001 and 2013, Isao Takahashi Power Electronics Award in 2010, Best Author Prize of the Society of Instrument and Control Engineers (SICE) in 2010, the Nagamori Grand Award in 2016, and First Prize Paper Award IEEE Transactions on Power Electronics in 2016. He is a Senior Member of IEE of Japan. He is also a member of the Society of Instrument and Control Engineers, Robotics Society of Japan, and Society of Automotive Engineers of Japan. He is an Associate Editor of the IEEE/ASME TRANSACTIONS ON MECHATRONICS from 2010 to 2014, IEEE Industrial Electronics Magazine from 2006, IEE of Japan Transactions on Industrial Application from 2013, and Transactions on SICE from 2013 to 2016. He is a Chairperson of the Society of Automotive Engineers of Japan (JSAE) vehicle electrification committee from 2014 and a past chairperson of IEEE/IES Technical Committee on Motion Control from 2012 to 2013.

Leonid M. Fridman received the M.S. degree in mathematics from Kuibyshev (Samara) State University, Samara, Russia, in 1976, the Ph.D. degree in applied mathematics from the Institute of Control Science, Moscow, Russia, in 1988, and the Dr.Sc. degree in control science from the Moscow State University of Mathematics and Electronics, Moscow, Russia, in 1998.

From 1976 to 1999, he was with the Department of Mathematics, Samara State Architecture and Civil Engineering University. From 2000 to 2002, he was with the Department of Postgraduate Study and Investigations, Chihuahua Institute of Technology, Chihuahua, Mexico. In 2002, he joined the Department of Control Engineering and Robotics, Division of Electrical Engineering of Engineering Faculty, National Autonomous University of Mexico, Mexico City, Mexico. His research interest includes variable structure systems. He has coauthored and has been a Co-Editor for ten books and 17 special issues devoted to the sliding mode control.

Prof. Fridman served from 2014 to 2018 as a Chair of Technical Committee (TC) on Variable Structure and Sliding Mode Control of IEEE Control Systems Society. He was a recipient of a Scopus prize for the best cited Mexican Scientists in Mathematics and Engineering 2010. He served and serves as an Associated Editor in different leading journals of control theory and applied mathematics. He was working as an Invited Professor in more than 20 universities and research laboratories of Argentina, Australia, Austria, China, France, Germany, Italy, Israel, and Spain. Actually he is also an International Chair of Institut National de Recherche en Informatique et en Automatique (INRIA), France, and a High-Level Foreign Expert of Ministry of Education of China.